Synthesis of *ortho*-carboxamidostilbene analogues and their antidiabetic activities through *in vitro* and *in silico* approaches

Babai Mahdi [iD] [1,2], **Mohamad Nurul Azmi** [iD][1,*], **Lacksany Phongphane** [iD][1],

Muhammad Solehin Abd Ghani [iD][1], **Mohamad Hafizi Abu Bakar** [iD][3],

Mohammad Tasyriq Che Omar [iD][4], **Andrey A. Mikhaylov** [iD] [5]

and Unang Supratman[iD] [6]

[1]Natural Products and Synthesis Organic Research Laboratory (NPSOLab), School of Chemical Sciences, Universiti Sains Malaysia, 11800 Minden, Penang, Malaysia
[2]Department of Chemistry, Nigerian Army University Biu, 1500, Biu, Borno State, Nigeria
[3]Bioprocess Technology Division, School of Industrial Technology, Universiti Sains Malaysia 11800 Minden, Penang, Malaysia; [4]Biological Section, School of Distance Education, Universiti Sains Malaysia, 11800 Minden, Penang, Malaysia
[5]Shemyakin-Ovchinnikov Institute of Bioorganic Chemistry of the Russian Academy of Sciences, 16/10 Miklukho-Maklaya St., Moscow, 117997 Russia
[6]Department of Chemistry, Faculty of Mathematics and Natural Sciences, Universitas Padjadjaran, 45363 Jatinangor, Indonesia

Abstract: Due to the recent emergence of drug-resistance of antidiabetic drugs and the increase in the number of diabetes cases around the world, the search for and discovery of more effective α-amylase inhibitors is of great interest. In the present study, a new series of eighteen *ortho*-carboxamidostilbene derivatives were synthesized via Heck coupling reaction. The structures of the synthesized compounds were identified by various spectroscopic techniques, including HREIMS, FTIR and 1D-NMR. In addition, the compounds were evaluated *in vitro* for their potential α-amylase inhibitory potency using acarbose as the reference drug. Compounds **5e**, **5f** and **6e** showed remarkably moderate to good inhibitory activity with IC_{50} values ranging from $13.3 - 28.2$ μM. These compounds showed potent IC_{50} values compared to the reference drug acarbose ($IC_{50} = 30.2 \pm 0.1$ μM). The *in silico* molecular docking studies revealed the binding interactions of the most active *ortho*-carboxamidostilbene derivatives (**5e** and **6e**) with binding energies of -8.7 $\pm$ 0.0 and -8.6 $\pm$ 0.2 kcal/mol, respectively. Based on the structure-activity relationship (SAR) analysis, it was established that variations in the inhibitory activities of α-amylase enzymes were attributed to distinct types of substituents at the amide group of the aryl ring A along with the number and position of methoxy groups attached to the aryl ring B. These findings highlight the α-amylase inhibitory properties of *ortho*-carboxamidostilbene containing cyclohexane and phenyl moieties, serving as potential lead compounds in antidiabetic drug development for the treatment of type II diabetes mellitus.

Keywords: *Ortho*-carboxamidostilbene; Heck coupling; diabetes; α-amylase; molecular docking. ©2024 ACG Publication. All rights reserved.

1. Introduction

Diabetes is one of the most prevalent health problems in the world.[1] The number of adult-onset diabetes cases has increased worldwide in recent years, and researchers are working to develop an effective treatment. Although there are different forms of diabetes, type I and type II are the most

common.[2,3] In type I diabetes, the body's immune system attacks and kills the cells in the pancreas that produce insulin.[4,5] In contrast, in type II diabetes, the body develops immunity to the action of insulin or does not produce enough of it to control blood glucose levels.[6,7] It has been suggested that by 2030, developing nations will account for the bulk of diabetic patients worldwide (77.6%).[1]

Furthermore, Bommer and co-researchers also reported that by 2030, the absolute cost of the global economy will increase from $1.3 trillion (95%) in 2015 to $2.2 trillion in the baseline scenario, $2.5 trillion in the prior trends' scenario, and $2.1 trillion in the target scenario.[8] This means that the cost of managing this disease will increase from 1.8% of global GDP in 2015 to a maximum of 2.2%.[8] The 10th edition of the International Diabetes Federation 2021 states that diabetes is one of the fastest-growing global health emergencies of the 21st century. It will affect 643 million people in 2030 and 783 million people in 2045.[9] More than 6.7 million people between the ages of 20 and 79 were expected to die because of diabetes in 2021. Every year, more children and adolescents (i.e. under the age of 19) are diagnosed with diabetes. In 2021, more than 1.2 million of them encountered type I diabetes. Diabetes has already caused around one trillion dollars in direct medical costs.[10]

When glucose uptake by Na/glucose co-transporter 1 (SGLT1) is excessive, mammalian pancreatic α-amylase severely restricts it. Additionally, it binds selectively to glycoprotein N-glycans in the brush border membrane to initiate starch digestion.[7] Consequently, α-amylase is an essential enzyme that catalyzes the initial stage of starch breakdown into glucose. The breakdown of starch and glycogen is aided by the enzyme α-amylase, which is being investigated as a potential target for problems related to the intake of carbohydrates, such as diabetes, obesity, dental caries and periodontal diseases.[12] It is an excellent target because some research has been done on this inhibitor and its relationship to type II diabetes mellitus.[13,14] Pancreatic α-amylase, which makes up a large amount of pancreatic fluid, is discharged from pancreatic acinar cells into the duodenum to break down starch and generate maltose or maltooligosaccharides. These are then further hydrolyzed by enzymes known as sucrase-isomaltose, which are brush border membrane (BBM) enzymes.[7] The glucose-end product is subsequently transported into enterocytes via Na/glucose co-transporter 1 (SGLT1) at the BBM.[7] Diabetes can be efficiently managed by lowering postprandial hyperglycemia and postponing glucose absorption through inhibition of certain enzymes that hydrolyze carbs, which primarily refer to α-glucosidase and α-amylase.[9,15] Recent studies on stilbene such as resveratrol and rosewood, can cure diabetes.[16,21,25] Pterostilbene has been demonstrated to be advantageous in animal models of diabetes and metabolic diseases.[17] Various studies reported the synthesis of a new series of *ortho*-carboxamidostilbene derivatives, which were evaluated for their cytotoxic effects as well as their *in vitro* and *in silico* ability to inhibit α-amylase and α-glucosidase enzymes.[3,18]

Therefore, in this project, we synthesized three series of *ortho*-carboxamidostilbene derivatives (i.e., 3,4,5-trimethoxy, 2,4-dimethoxy and 2,5-dimethoxy series) with six different substitutions at the amide group. All synthesized derivatives were evaluated against α-amylase enzyme via *in vitro* technique. In addition, molecular docking studies of the active compounds were carried out to understand the binding interactions of the most active analogues with the enzyme binding site. Furthermore, structure-activity relationships (SAR) were performed to find relationships between chemical structure (or structural-related properties) and biological activity (or target property) of synthesized compounds.

2. Experimental

2.1. Chemical Material and Apparatus

All reactions were performed under reflux in dried glassware under a nitrogen gas (N_2) atmosphere. Liquid transfers were performed with standard syringes. Unless otherwise stated, the chemicals and reagents used were of the highest purity. They were obtained from Sigma-Aldrich Co., Acros Organics, and Merck Chemical Co. and were used without further purification. *N,N*-dimethylformamide (DMF, QReC, AR grade) was dried over 4Å molecular sieves. Tetrahydrofuran (THF) was dried by heating under reflux over sodium metal in the presence of benzophenone as an indicator. Weighing was performed on electronic analytical balance. Column chromatography was performed using Merck silica gel (0.040-0.063 mm). For thin-layer chromatography, a TLC aluminum

Synthesis and antidiabetic activity and *in silico* study of *ortho*-carboxamidostilbene analogues

sheet precoated with silica gel (silica gel 60 F$_{254}$) was used and visualized under UV (λ_{max} = 254 nm and/or 366 nm). The ^{1}H NMR and ^{13}C NMR spectra were recorded using a Bruker Advance spectrometer (500 MHz for ^{1}H NMR and 125 MHz for ^{13}C NMR, Bruker Bioscience, Billerica, MA, USA). Chemical shifts were referenced to TMS or the residual solvent (CDCl$_3$ = 7.26 ppm for ^{1}H and 77.0 ppm for ^{13}C spectroscopy; Acetone-d$_6$ = 2.05 ppm for ^{1}H and 29.9, 206.7 ppm for ^{13}C spectroscopy). Fourier transform infrared (FT-IR) spectra were recorded by Perkin Elmer FT-IR spectroscopy (Perkin Elmer, Waltham, MA, USA) in the frequency range of 4000 – 400 cm^{-1} using the ATR method. The mass spectra (HREIMS) were recorded with a Waters Xevo QTOF MS (Milford, MA, USA). Melting points were measured using an open capillary tube by Stuart Scientific SMP10 melting point apparatus (Staffordshire, UK) in temperatures ranging from 25 °C to 350 °C.

2.2. Chemistry

2.3.1. General Procedure for the Synthesis of Styrenes

In a stirred solution of methyl triphenyl phosphonium bromide (1.5 equiv) in dry THF (60 mL) under an argon gas atmosphere at -75 °C, potassium *tert*-butoxide (*tert*-BuOK, 1.5 equiv.) and benzaldehyde analogues (1 equiv.) were added. The dry ice (ice bath) was removed after 40 min and the resulting mixture was stirred at room temperature for 24 hrs, then quenched with 10 mL aqueous ammonium chloride (NH$_4$Cl). The mixture was extracted with ethyl acetate (EtOAc) (3 × 20 mL). The organic layers were combined and dried by the addition of anhydrous sodium sulfate (Na$_2$SO$_4$), which then filtered and evaporated under reduced pressure to give the crude product. Chromatography on silica gel eluted with 100% hexane gave the desired product (Supporting information, S3-S4).

2.2.2. General Procedure for the Synthesis of N-(2-iodophenyl)acylamides

To a stirred, cooled (0-5 °C) solution of 2-iodoaniline (2.0 equiv.) in 40 mL THF and triethylamine (Et$_3$N) (3.0 equiv.), the acyl chlorides (3.0 equiv.) in 5 mL THF was added dropwise and the ice bath was removed. The resulting mixture was stirred vigorously for 6 hrs at room temperature. The solid Et$_3$N.HCl was filtered and the resulting filtrate was washed with THF (3 × 5 mL). The organic layers were combined, followed by the removal of THF under reduced pressure to give the corresponding amide as a white solid (Supporting information, S4-S5).[19-21]

2.2.3. General Procedure for Heck Reactions

In a two-neck round bottom flask, *N*-(2-iodophenyl)acylamide (1.0 equiv.) was dissolved in 12 mL of dry DMF and stirred under N$_2$. The solution was heated to 120 °C and reflux for 15 min. The palladium (II) acetate (1.0 equiv.) and Et$_3$N (5.0 equiv.) were added into the reaction flask, followed by styrene (1.2 equiv.). The mixture was stirred and heated at 120 °C under N$_2$ until all the amides had been consumed. The reaction was stopped, allowed to cool and later quenched with NH$_4$Cl. The mixture was then extracted with 40 mL EtOAc and concentrated under reduced pressure. The crude residue was purified by column chromatography (silica gel, *n*-hexane-EtOAc mixture) to afford the coupling products.[19-21]

2.2.3.1. Synthesis of N-2-(3,4,5-trimethoxy)carboxamido Stilbenes

(E)-N-(2-(3,4,5-trimethoxystyryl)phenyl)acetamide (5a): White solid. Yield: 40 %; m.p. 190−192 °C; R_f ≈ 0.5 [UV-active, *n*-Hexane/EtOAc (Purple spot)]. IR ν_{max}: 3230 (N-H), 2929 (C−H), 1645 (C=O), 1570 (C=C), 1455, 1240, 1125, 1009, 740. ^{1}H NMR (500 MHz, CDCl$_3$) δ ppm: 7.84 (d, *J* = 8.0 Hz, H−6′, 1H), 7.53 (d, *J* = 8.0 Hz, H−3′, 1H), 7.34 (t, *J* = 8.0 Hz, H−4′, 1H), 7.21 (t, *J* = 8.0 Hz, H−5′, 1H), 7.17 (s, N-H, 1H), 7.06 (d, *J* = 16.0 Hz, H−8, 1H), 6.96 (d, *J* = 16.0 Hz, H−7, 1H), 6.74 (s, H−2, H−6, 2H), 3.93 (s, H−9, 6H), 3.90 (s, H−10, 3H), 2.25 (s, H−2′′, 3H). ^{13}C NMR (125 MHz, CDCl$_3$) δ ppm: 168.7 (C−1′′), 153.4 (C−3, C−5), 138.3 (C−1′), 134.6 (C−4), 132.8 (C−1), 132.4 (C−2′), 130.5 (C−3′), 128.3 (C−5′), 126.9 (C−7), 125.7 (C−4′), 124.4 (C−6′), 123.2 (C−8), 103.9 (C−2,C−6), 61.0 (C−10), 56.2 (C−9), 24.28 (C−2′′). HREIMS (TOF-ES$^+$) *m/z* 350.1364 [M+Na]$^+$ (calculated for C$_{19}$H$_{21}$NO$_4$Na 350.1368).

(E)-N-(2-(3,4,5-trimethoxystyryl)butyramide (5b): White solid. Yield: 70 %. m.p.152−154 °C. $R_f \approx 0.2$ [UV-active, *n*-Hexane/EtOAc (Purple spot)]. IR ν_{max}: 3239 (N-H), 2945 (C-H) 1645 (C=O), 1580 (C=C), 1415 (C-H bend), 1235 (C-N), 1130, 990, 755. ^{1}H NMR (500 MHz, CDCl$_3$) δ ppm: 7.82 (d, *J* = 7.8 Hz, H−6′, 1H), 7.54 (d, *J* = 7.8 Hz, H−3′, 1H), 7.32 (t, *J* = 7.8 Hz, H−4′, 1H), 7.21 (t, *J* = 7.5 Hz, H−5′, 1H), 7.15 (s, N-H, 1H), 7.07 (d, *J* = 16.0 Hz, H−8, 1H), 6.96 (d, *J* = 16.0 Hz, H−7, 1H), 6.73 (s, H−2, H−6, 2H), 3.93 (s, H−9, 6H), 3.90 (s, H−10, 3H), 2.42 (t, *J* = 7.4 Hz, H−2″, 2H), 1.84 (q, *J* = 7.3 Hz, H−3″, 2H), 1.08 (t, *J* = 7.3 Hz, H−4″, 3H). ^{13}C NMR (125 MHz, CDCl$_3$) δ ppm: 171.4 (C−1″), 153.4 (C−3, C−5), 138.3 (C−4), 134.5 (C−1′), 132.7 (C−1), 132.5 (C−2′), 130.4 (C−3′), 128.39 (C−5′), 126.9 (C−4′), 125.6 (C−7), 124.4 (C−8), 123.1 (C−6′), 103.7 (C−2, C−6), 61.0 (C−10), 56.1 (C−9), 39.5 (C−2″), 19.37 (C−3″), 13.8 (C−4″). HREIMS (TOF-ES$^+$) *m/z* 378.1689 [M+Na]$^+$ (calculated for C$_{21}$H$_{25}$NO$_4$Na: 378.1784).

(E)-N-(2-(3,4,5-trimethoxystyryl)phenyl)isobutyramide (5c): White solid. Yield: 35 %; m.p. 132−134 °C. $R_f \approx 0.3$ [UV-active, *n*-Hexane/EtOAc (Purple spot)]. IR ν_{max}: 3359 (N-H), 2934 (C-H), 1650 (C=O), 1499 (C=C), 1449 (C-H bend), 1329, 1229, 1119, 975, 752. ^{1}H NMR (500 MHz, CDCl$_3$) δ ppm: 7.77 (d, *J* = 7.8 Hz, H−6′, 1H), 7.52 (d, *J* = 7.8 Hz, H−3′, 1H), 7.29 (t, *J* = 7.8 Hz, H−5′, 1H), 7.20 (d, *J* = 7.8 Hz, H−4′, 2H), 7.03 (d, *J* = 16.0 Hz, H−8, 1H), 6.92 (d, *J* = 16.0 Hz, H−7, 1H), 6.71 (s, H−2, H−6, 2H), 3.89 (s, H−9, 6H), 3.87 (s, H−10, 3H), 2.59 (m, H−2″, 1H), 1.30 (d, *J* = 7.0 Hz, H−3″, 6H). ^{13}C NMR (125 MHz, CDCl$_3$) δ ppm: 175.3 (C−7′), 153.4 (C−3,C−5), 138.3 (C−2′), 134.5 (C−4), 132.8 (C−1), 132.3 (C−1′), 130.6 (C−6′), 128.3 (C−4′), 126.8 (C−7), 125.6 (C−5′), 124.5 (C−3′), 123.1 (C−8), 103.6 (C−2,C−6), 61.0 (C−10), 56.1 (C−9), 36.4 (C−2″), 19.7 (C−3″). HREIMS (TOF-ES$^+$) *m/z* 402.1301 [M+Na]$^+$ (calculated for C$_{21}$H$_{25}$NO$_4$Na: 402.1317).

(E)-N-(2-(3,4,5-trimethoxystyryl)phenyl)furan-2-carboxamide (5d): White solid. Yield: 80 %. m.p. 125−127 °C. $R_f \approx 0.3$ [UV-active, *n*-Hexane/EtOAc (Purple spot)]. IR ν_{max}: 3285 (N-H), 3134 (C-H), 2929, 1645 (C=O), 1585 (C=C), 1504, 1449 (C-H bend), 1284 (C-N), 1160, 1004, 740. ^{1}H NMR (500 MHz, CDCl$_3$) δ ppm: 8.16 (s, N-H, 1H), 8.03 (d, *J* = 8.0 Hz, H−6′, 1H), 7.54 (d, *J* = 8.0 Hz, H−3′, 1H), 7.50 (d, *J* = 2.0 Hz, H−4″, 1H), 7.34 (t, *J* = 8.0 Hz, H−5′, 1H), 7.27 (d, *J* = 3.5 Hz, H−2″, 1H), 7.22 (t, *J* = 8.0 Hz, H−4′, 1H), 7.13 (d, *J* = 16.0 Hz, H−8, 1H), 6.98 (d, *J* = 16.0 Hz, H−7, 1H), 6.74 (s, H−2, H−6, 2H), 6.57 (dd, *J* = 3.5, 2.0 Hz, H−3″, 1H), 3.90 (s, H−9, 6H), 3.88 (s, H−10, 3H). ^{13}C NMR (125 MHz, CDCl$_3$) δ ppm: 156.2 (C−7′), 153.5 (C−3,C−5), 147.9 (C−1″), 144.3 (C−4″), 138.4 (C−4), 134.0 (C−1′), 132.9 (C−3′), 132.8 (C−2′), 130.0 (C−1), 128.4 (C−5′), 127.2 (C−7), 125.5 (C−8), 123.5 (C−4′), 122.9 (C−6′), 115.4 (C−2″), 112.7 (C−3″), 103.8 (C−2,C−6), 61.0 (C−10), 56.2 (C−9). HREIMS (TOF-ES$^+$) *m/z* 402.1301 [M+Na]$^+$ (calculated for C$_{22}$H$_{21}$NO$_5$Na: 402.1317).

(E)-N-(2-(3,4,5-trimethoxystyryl)phenyl)cyclohexane carboxamide (5e): White solid. Yield: 35 %. m.p. 194−196 °C. $R_f \approx 0.5$ [UV-active, *n*-Hexane/EtOAc (Purple spot)]. IR ν_{max}: 3278 (N-H), 2917 (C-H), 2846, 1643 (C=O), 1513 (C=C), 1229, 1129, 964, 805. ^{1}H NMR (500 MHz, CDCl$_3$) δ ppm: 7.71 (d, *J* = 7.8 Hz, H−6′, 1H), 7.46 (d, *J* = 7.8 Hz, H−3′, 1H), 7.23 (t, *J* = 7.8 Hz, H−5′, 1H), 7.13 (t, *J* = 7.8 Hz, H−4′, 1H), 7.07 (s, N−H, 1H), 6.98 (d, *J* = 16.0 Hz, H−8, 1H), 6.86 (d, *J* = 16.0 Hz, H−7, 1H), 6.65 (s, H−2, H−6, 2H), 3.83 (s, H−9, 6H), 3.81 (s, H−10, 3H), 2.25 (m, H−1″, 1H), 1.97 (m, H−4″, 2H), 1.78-1.64 (m, H−2, H−6, 4H), 1.32 − 1.16 (m, H−3″, H−5″, 4H). ^{13}C NMR (125 MHz, CDCl$_3$) δ ppm: 174.4 (C−7′), 153.4 (C−3, C−4), 138.2 (C−4), 134.5 (C−1′), 132.8 (C−1), 132.1 (C−2′), 130.7 (C−3′), 128.3 (C−5′), 126.7 (C−7), 125.7 (C−8), 124.6 (C−4′), 123.2 (C−6′), 103.6 (C−2, C−6), 61.0 (C−10), 56.1 (C−9), 46.2 (C−1″), 29.9 (C−2″,C−6″), 25.7 (C−3″,C−5″), 25.6 (C−4″). HREIMS (TOF-ES$^+$) *m/z* 418.1990 [M+Na]$^+$ (calculated for C$_{24}$H$_{29}$NO$_4$Na: 418.1994).

(E)-N-(2-(3,4,5-trimethoxystyryl)phenyl)benzamide (5f): White solid. Yield: 52 %; m.p. 158−160 °C. $R_f \approx 0.6$ [UV-active, *n*-Hexane/EtOAc (Purple spot)]. IR ν_{max}: 3215 (N-H), 2929 (C-H), 3110, 1640 (C=O), 1575 (C=C), 1504, 1235, 1125, 1004. ^{1}H NMR (500 MHz, CDCl$_3$) δ ppm: 7.98 (s, N−H, 1H), 7.93 (d, *J* = 7.8 Hz, H−2″, H−6″, 2H), 7.89 (s, H−6′, 1H), 7.59 (d, *J* = 7.8 Hz, H−3″, H−5″, 2H), 7.53 (d, *J* = 7.8 Hz, H−4′, H−5′, 2H), 7.38 (t, *J* = 7.8 Hz, H−4′, 1H), 7.26 (d, *J* = 7.8 Hz, H−3′, 1H), 7.14 (d, *J* = 16.0 Hz, H−8, 1H), 7.01 (d, *J* = 16.0 Hz, H−7, 1H), 6.72 (s, H−2, H−6, 2H), 3.89 (d, *J* = 1.1 Hz, H−9, 6H, H−10, 3H). ^{13}C NMR (125 MHz, CDCl$_3$) δ ppm: 165.7 (C−7′), 153.4 (C−3,C−5), 138.4 (C−4), 134.7 (C−1′), 134.6 (C−1), 132.9 (C−1″), 132.7 (C−4″), 132.0 (C−2′), 130.6 (C−3′), 128.9 (C−3″,C−5″), 128.4 (C−5′), 127.2 (C−2″,C−6″), 125.8 (C−7), 124.3 (C−4′), 123.1 (C−6′), 103.7 (C−2,C−6), 61.0

Synthesis and antidiabetic activity and *in silico* study of *ortho*-carboxamidostilbene analogues

(C−10), 56.1 (C−9). HREIMS (TOF-ES$^+$) *m/z* 412.1523 [M+Na]$^+$ (calculated for C$_{24}$H$_{23}$NO$_4$Na: 412.1525).

2.2.3.2. Synthesis of N-2-(2,4-dimethoxy)carboxamido Stilbenes

(E)-N-(2-(2,4-dimethoxystyryl)phenyl)acetamide (6a): White solid. Yield: 50 %. m.p. 115−118 °C. R_f ≈ 0.3 [UV-active, *n*-Hexane/EtOAc (Purple spot)]. IR ν$_{max}$: 3270 (N-H), 2924 (C-H str), 2830, 1650 (C=O), 1504, 1284, 1200, 1030, 750. ^{1}H NMR (500 MHz, Acetone-d$_6$) δ ppm: 8.82 (s, N−H, 1H), 7.76 (d, *J* = 8.0 Hz, H−6′, 1H), 7.63 (d, *J* = 8.2 Hz, H−6, 1H), 7.57 (d, *J* = 8.2 Hz, H−3′, 1H), 7.35 (d, *J* = 16.0 Hz, H−7, 1H), 7.31 (d, *J* = 16.0 Hz, H−8 1H), 7.27 (s, H−5, 1H), 7.25 (t, *J* = 8.2 Hz, H−4′, 1H), 7.16 (t, *J* = 8.2 Hz, H−5′, 1H), 6.62 (d, *J* = 8.0 Hz, H−2, 1H), 6.58 (d, *J* = 8.0 Hz, H−3, 1H), 3.91 (s, 3H), 3.85 (s, 3H), 2.18 (s, 3H). ^{13}C NMR (125 MHz, CDCl$_3$) δ ppm: 168.6 (C−1″), 160.9 (C−4), 158.2 (C−2), 134.4 (C−1′), 130.9 (C−2′), 128.9 (C−3′), 127.8 (C−5′), 127.7 (C−7), 127.53 (C−4′), 126.9 (C−6), 125.3 (C−8), 123.8 (C−1), 121.8 (C−5), 119.8 (C−6′), 105.0 (C−5), 98.4 (C−3), 55.4 (C−10), 24.5 (C−2). HREIMS (TOP-ES$^+$) *m/z* 320.1266 [M+Na]$^+$ (calculated for C$_{18}$H$_{19}$NO$_3$Na: 320.1262).

(E)-N-(2-(2,4-dimethoxystyryl)phenyl)butyramide (6b): White solid. Yield: 65 %. m.p. 126−128 °C. R_f ≈ 0.6 [UV-active, *n*-Hexane/EtOAc (Purple spot)]. IR ν$_{max}$: 3249 (N-H), 2929 (C-H str), 2824, 1640 (C=O), 1600 (C=C), 1455, 1279, 1200, 1030, 960, 740. ^{1}H NMR (500 MHz, CDCl$_3$) δ ppm: 7.91 (d, *J* = 8.0 Hz, H−6, 1H), 7.50 (d, *J* = 7.8 Hz, H−6′, 1H), 7.49 (d, *J* = 7.8 Hz, H−3′, 1H), 7.27 (d, *J* = 7.8 Hz, H−4′, 1H), 7.24 (d, *J* = 16.0 Hz, H−8, 1H), 7.14 (t, *J* = 8.0 Hz, H−5, 1H), 7.05 (d, *J* = 16.0 Hz, H−7), 6.53 (d, *J* = 8.0 Hz, H−5, 1H), 6.48 (s, H−3, 1H), 3.88 (s, H−10, 3H), 3.86 (s, H−9, 3H), 2.37 (t, *J* = 7.0 Hz, H−2″, 2H), 1.80 (m, H−3″, 2H), 1.03 (t, *J* = 7.0 Hz, H−4″, 3H). ^{13}C NMR (125 MHz, CDCl$_3$) δ ppm: 171.3 (C−7′), 160.9 (C−4), 158.2 (C−2), 134.4 (C−2′), 130.6 (C−6), 127.8 (C−1), 127.7 (C−1′), 127.0 (C−6′), 125.1 (C−4′), 123.4 (C−7), 121.9 (C−5′), 119.2 (C−3′), 104.9 (C−5), 98.5 (C−3), 55.5 (C−9), 55.4 (C−10), 39.6 (C−8′), 19.2 (C−9′), 13.8 (C−10′). HREIMS (TOF-ES$^+$) *m/z* 348.1577 [M+Na]$^+$ (calculated for C$_{20}$H$_{23}$NO$_3$Na: 348.1576).

(E)-N-(2-(2,4-dimethoxystyryl)phenyl)isobutyramide (6c): White solid. Yield: 58 %. m.p. 144−146 °C. R_f ≈ 0.6 [UV-active, *n*-Hexane/EtOAc (Purple spot)]. IR ν$_{max}$: 3242 (N-H), 3053 (C-H), 2966 (C-H), 1645 (C=O), 1525 (C=C), 1449, 1284, 1195, 1025, 819, 740. ^{1}H NMR (500 MHz, CDCl$_3$) δ ppm: 7.94 (d, *J* = 8.0 Hz, H−6′, 1H), 7.50 (d, *J* = 7.8 Hz, H−4, 1H), 7.45 (d, *J* = 8.0 Hz, H−3′, 1H), 7.27 (s, H−3, 1H), 7.22 (d, *J* = 16.5 Hz, H−8, 1H), 7.14 (t, *J* = 7.8 Hz, H−5′, 1H), 7.06 (d, *J* = 16.5 Hz, H−7, 1H), 6.53 (d, *J* = 8.0 Hz, H−5, 1H), 6.49 (d, *J* = 7.8 Hz, H−4′, 1H), 3.86 (s, H−10, 3H), 3.84 (s, H−1, 3H), 2.57 (m, H−2″, 1H), 1.30 (d, *J* = 7.0, H−3″ Hz, 6H). ^{13}C NMR (125 MHz, CDCl$_3$) δ ppm: 176.9 (C−1″), 160.2 (C−4), 156.4 (C−2), 143.5 (C−1′), 130.3 (C−6), 127.5 (C−2′), 125.6 (C−3′), 124.9 (C−5), 123.9 (C−7), 117.3 (C−6′), 105.9 (C−5), 98.4 (C−3), 55.5 (C−9), 55.3 (C−10), 29.7 (C−2″), 24.3 (C−3″). HREIMS (TOF-ES$^+$) *m/z* 348.1575 [M+Na]$^+$ (calculated for C$_{20}$H$_{23}$NO$_3$Na: 348.1576).

(E)-N-(2-(2,4-dimethoxystyryl)phenyl)furan-2-carboxamide (6d): White solid. Yield: 64 %. m.p.125−127 °C. R_f ≈ 0.5 [UV-active, *n*-Hexane/spot]. IR ν$_{max}$: 3280 (N-H), 2984 (C-H), 1645 (C=O), 1507, 1475, 1160, 1099, 1020, 827, 748, 661. ^{1}H NMR (500 MHz, CDCl$_3$) δ ppm: 8.13 (s, N−H, 1H), 8.00 (d, *J* = 9.0 Hz, H−6′, 1H), 7.51 (d, *J* = 8.5 Hz, H−6, 1H), 7.43 (d, *J* = 1.8 Hz, H−2″, 1H), 7.42 (d, *J* = 8.5 Hz, H−3′, 1H), 7.24 (t, *J* = 8.5 Hz, H−4′, 1H), 7.21 (t, *J* = 8.5 Hz, H−5′, 1H), 7.13 (d, *J* = 3.5 Hz, H−4″, 1H), 7.10 (d, *J* = 9.0 Hz, H−5, 1H), 6.50 (d, *J* = 3.5, 1.8 Hz, H−3″, 1H), 6.47 (d, *J* = 2.4 Hz, H−3, 1H), 6.45 (d, *J* = 16.5, H−7, H−8, Hz, 2H), 3.78 (s, H−10, 3H), 3.87 (s, H−9, 3H). ^{13}C NMR (125 MHz, CDCl$_3$) δ ppm: 160.9 (C−7′), 158.3 (C−4), 156.2 (C−1″), 148.0 (C−4″), 144.2 (C−2), 133.8 (C−1′), 130.7 (C−6), 128.1 (C−2′), 128.0 (C−3′), 127.8 (C−5′), 127.0 (C−7), 125.3 (C−4′), 123.1 (C−6′), 121.4 (C−2″), 119.2 (C−8), 115.2 (C−3″), 112.5 (C−1), 104.9 (C−5), 98.5 (C−3), 55.4 (C−9), 55.4 (C−10). HREIMS (TOF-ES$^+$) *m/z* 372.1223 [M+Na]$^+$ (calculated for C$_{21}$H$_{19}$NO$_4$Na: 372.1212).

(E)-N-(2-(2,4-dimethoxystyryl)phenyl)cyclohexane carboxamide (6e): White solid. Yield: 40 %. m.p. 157−159 °C. R_f ≈ 0.63 [UV-active, *n*-Hexane/EtOAc (Purple spot)]. IR ν$_{max}$: 3275 (N-H), 2929 (C-H), 2850, 1645 (C=O), 1525, 1444, 1279, 1200, 949, 725. ^{1}H NMR (500 MHz, CDCl$_3$) δ ppm: 7.96 (d, *J* = 8.5 Hz, H−6, 1H), 7.53 (t, *J* = 7.8 Hz, H−5′, 1H), 7.48 (d, *J* = 7.8 Hz, H−6′, 1H), 7.34 (t, *J* = 7.8 Hz, H−4′, 1H), 7.22 (d, *J* = 16.5 Hz, H−8, 1H), 7.17 (d, *J* = 7.8 Hz, H−3′, 1H), 7.11 (s, N−H, 1H), 7.09 (d, *J*

= 16.5 Hz, H−7, 1H), 6.57 (d, *J* = 8.5 Hz, H−5, 1H), 6.52 (d, *J* = 2.4 Hz, H−3, 1H), 3.89 (s, H−9, 3H), 3.87 (s, H−10, 3H), 2.31 (m, H−1″, 1H), 2.07−1.95 (m, H−2″, H−6″, 4H), 1.76−1.53 (m, H−3″, H−5″, 4H), 1.32 (m, H−4″, 2H).^{13}C NMR (125 MHz, CDCl$_3$) δ ppm: 174.4 (C−7′), 161.0 (C−4), 158.4 (C−2), 134.6 (C−6′), 130.8 (C−6), 129.1 (C−1′), 127.9 (C−2′), 127.1 (C−4), 125.2 (C−7), 124.1 (C−3′), 123.5 (C−5′), 122.0 (C−1), 119.8 (C−8), 105.2 (C−5), 98.7 (C−3), 56.0 (C−9), 55.6 (C−10), 46.7 (C−1″), 29.9 (C−2″,C−6″), 29.6 (C−4″), 25.8 (C−3″,C−5″). HREIMS (TOF-ES$^+$) *m/z* 388.1895 [M+Na]$^+$ (calculated for C$_{23}$H$_{27}$NO$_3$Na: 388.1889).

*(E)-N-(2-(2,4-dimethoxystyryl)phenyl)benzamide (**6f**)*: White solid. Yield: 49 %. m.p. 169−171 °C. $R_f \approx$ 0.6 [UV-active, *n*-Hexane/EtOAc (Purple spot)]. IR ν$_{max}$: 3225 (N-H), 3019, 2945 (C-H), 1640 (C=O), 1580, 1444, 1260, 1195, 1025, 954, 815, 679; ^{1}H NMR (500 MHz, CDCl$_3$) δ ppm: 8.10 (d, *J* = 8.0 Hz, H−6, 1H), 8.01 (s, N-H, 1H), 7.94 (d, *J* = 7.5 Hz, H−2″, H−6″, 2H), 7.58 (t, *J* = 7.5 Hz, H−4″, 1H), 7.52 (t, *J* = 7.5 Hz, H−3″, H−5″, 2H), 7.47 (d, *J* = 8.0 Hz, H−3′, 1H), 7.34 (t, *J* = 8.0 Hz, H−4′, 1H), 7.27 (d, *J* = 16.2 Hz, H−8, 1H), 7.23 (t, *J* = 8.0 Hz, H−5′, 1H), 7.19 (d, *J* = 16.2 Hz, H−7, 1H), 6.54 (d, *J* = 8.0 Hz, H−5, 1H), 6.50 (d, *J* = 2.4 Hz, H−3, 1H), 3.85 (s, H−9, 3H), 3.83 (s, H−10, 3H). ^{13}C NMR (125 MHz, CDCl$_3$) δ ppm: 160.9 (C−7′), 158.3 (C−4), 134.9 (C−2), 134.5 (C−1′), 131.8 (C−1″), 131.0 (C−4″), 128.8 (C−3″,5″), 128.3 (C−2′), 128.2 (C-6), 127.8 (C−3′), 127.2 (C−5), 127.1 (C−2″,6″), 125.3 (C−7″), 123.3 (C−4′), 121.8 (C−6′), 119.1 (C−8), 104.9 (C−1), 98.5 (C−3), 55.4 (C−9), 55.3 (C−10). HREIMS (TOF-ES$^+$) *m/z* 382.1414 [M+Na]$^+$ (calculated for C$_{23}$H$_{21}$NO$_3$Na: 382.1419).

2.2.3.3. Synthesis of N-2-(2,5-dimethoxy)carboxamido Stilbenes

*(E)-N-(2-(2,5-dimethoxystyryl)phenyl)acetamide (**7a**)*: White solid. Yield: 40 %; m.p. 169 – 171°C. $R_f \approx$ 0.4 [UV-active, *n*-Hexane/EtOAc (Purple spot)]. IR ν$_{max}$: 3290 (N-H), 2925 (C-H), 2830, 1645 (C=O), 1490, 1210, 1045, 965, 750. ^{1}H NMR (500 MHz, CDCl$_3$) δ ppm: 7.89 (d, *J* = 7.8 Hz, H−6′, 1H), 7.56 (d, *J* = 7.8 Hz, H−3′, 1H), 7.34 (d, *J* = 8.5 Hz, H−4, 1H), 7.28 (s, N-H, 1H), 7.18 (t, *J* = 7.8 Hz, H−4′, H−5′, 2H), 7.13 (d, *J* = 16.0 Hz, H−8, 1H), 7.14 (d, *J* = 16.0 Hz, H−7, 1H), 6.89 (d, *J* = 8.5 Hz, H−6, 1H), 6.86 (d, *J* = 8.5 Hz, H−3, 1H), 3.86 (s, H−9, 3H), 3.84 (s, H−10, 3H), 2.24 (s, H−2″, 3H). ^{13}C NMR (125 MHz, CDCl$_3$) δ ppm: 168.9 (C−1″), 153.7 (C−5), 151.6 (C−2), 134.6 (C−1′), 130.4 (C−2′), 128.2 (C−3′), 127.6 (C−5′), 127.2 (C−7), 126.9 (C−4′), 125.4 (C−6′), 124.4 (C−3), 123.9 (C−1), 113.8 (C−4), 112.5 (C−8), 112.1 (C−6), 56.1 (C−9), 55.8 (C−10), 24.3 (C−2″). HREIMS (TOF-ES$^+$) *m/z* 320.1255 [M+Na]$^+$ (calculated for C$_{18}$H$_{19}$NO$_3$Na: 320.1263).

*(E)-N-(2-(2,5-dimethoxystyryl)phenyl)butyramide (**7b**)*: White solid. Yield: 42 %. m.p. 149 – 151 °C. $R_f \approx$ 0.4 [UV-active, *n*-Hexane/EtOAc (Purple spot)]. IR ν$_{max}$: 3264 (N-H), 2924 (C-H), 2830, 1650 (C=O), 1604, 1499, 1274, 1200, 1045, 750. ^{1}H NMR (500 MHz, CDCl$_3$) δ ppm: 7.90 (d, *J* = 8.0 Hz, H−6′, 1H), 7.53 (d, *J* = 8.0 Hz H−3′, 1H), 7.30 (d, *J* = 16.5 Hz, H−7, 1H), 7.26 (t, *J* = 8.0 Hz, H−4′, H−5′, 2H), 7.17 (s, N-H, 1H), 7.13 (d, *J* = 16.5 Hz, H−8, 1H), 7.09 (d, *J* = 2.5 Hz, H−6, 1H), 6.86 (d, *J* = 8.5 Hz, H−3, 1H), 6.84 (dd, *J* = 8.5, 2.5 Hz, H−4, 1H), 3.84 (s, H−10, 3H), 3.80 (s, H−9, 3H), 2.38 (t, *J* = 7.5 Hz, H−2″, 2H), 1.80 (m, H−3″, 2H), 1.03 (t, *J* = 7.5 Hz, 3H). ^{13}C NMR (125 MHz, CDCl$_3$) δ ppm: 171.3 (C−1″), 153.7 (C−5), 151.6 (C−2), 134.6 (C−1′), 130.2 (C−2′), 128.2 (C−3′), 127.7 (C−5′), 127.2 (C−7), 126.8 (C−4′), 125.2 (C−6′), 124.4 (C−1), 123.6 (C−3), 113.0 (C−4), 112.4 (C−8), 112.1 (C−6), 56.1 (C−9), 55.8 (C−10), 39.6 (C−2″), 19.2 (C−3″), 13.8 (C−4″). HREIMS (TOF-ES$^+$) *m/z* 348.1579 [M+Na]$^+$ (calculated for C$_{20}$H$_{23}$NO$_3$Na: 348.1576).

*(E)-N-(2-(2,5-dimethoxystyryl) phenyl)isobutyramide (**7c**)*: White solid. Yield: 77 %. m.p. 190 – 191 °C. $R_f \approx$ 0.6 [UV-active, *n*-Hexane/EtOAc (Purple spot)]. IR ν$_{max}$: 3249 (N-H), 2969 (C-H), 2835, 1650 (C=O), 1485, 1284, 1185, 1020, 710. ^{1}H NMR (500 MHz, CDCl$_3$) δ ppm: 7.91 (d, *J* = 7.8 Hz, H−6′, 1H), 7.53 (d, *J* = 7.8 Hz, H−3′, 1H), 7.31 (s, N-H, 1H), 7.29 (d, *J* = 8.0 Hz, H−4′, 1H), 7.28 (d, *J* = 8.0 Hz, H−5′, 1H), 7.17 (s, H−6, 1H), 7.12 (d, *J* = 17.5 Hz, H−7, H−8, 2H), 6.86 (d, *J* = 8.5 Hz, H−3, 1H), 6.85 (dd, *J* = 8.5, 2.7 Hz, H−4, 1H), 3.86 (s, H−9, 3H), 3.83 (s, H−10, 3H), 2.57 (m, H−2″, 1H), 1.30 (d, *J* = 7.0 Hz, H−3″, 6H). ^{13}C NMR (125 MHz, CDCl$_3$) δ ppm: 175.2 (C−1″), 153.7 (C−5), 151.6 (C−2), 134.7 (C−1′), 130.2 (C−2′), 128.2 (C−3′), 127.7 (C−5′), 127.3 (C−7), 126.8 (C−4′), 125.1 (C−4), 124.4

Synthesis and antidiabetic activity and *in silico* study of *ortho*-carboxamidostilbene analogues

(C−6′), 123.5 (C−1), 114.0 (C−3), 112.3 (C−8), 112.2 (C−6), 56.1 (C−9), 55.8 (C−10), 36.6 (C−2″), 19.7 (C−3″). HREIMS (TOF-ES⁺) *m/z* 348.1583 [M+Na]⁺ (calculated for $C_{20}H_{23}NO_3Na$: 348.1576).

(E)-N-(2-(2,5-dimethoxystyryl) phenyl)furan-2-carboxamide (7d): White solid. Yield: 55 %. m.p. 128 ‒ 130 °C $R_f ≈$ 0.5 [UV-active, *n*-Hexane/ EtOAc (Purple spot)]. IR ν$_{max}$: 3294 (N-H), 2940 (C-H), 2830, 1650 (C=O), 1490, 1305, 1205, 1020, 740, 590. ¹H NMR (500 MHz, CDCl₃) δ ppm: 8.18 (s, N-H, 1H), 8.06 (d, *J* = 8.0 Hz, H−6′, 1H), 7.60 (d, *J* = 8.0 Hz, H−4, 1H), 7.50 (d, *J* = 1.8 Hz, H−4″, 1H), 7.37 (d, *J* = 16.0 Hz, H−7, 1H), 7.31 (d, *J* = 16 .0 Hz, H−8, 1H), 7.26 (d, *J* = 8.0 Hz, H−3′, 1H), 7.26 (d, *J* = 8.0 Hz, H−4′, 1H), 7.12 (d, *J* = 2.5 Hz, H−6, 1H), 6.87 (d, *J* = 9.0, H−3, 1H), 6.84 (d, *J* = 9.0, H−5′, 1H), 6.56 (dd, *J* = 3.5, 1.8 Hz, H−3″, 1H), 3.85 (s, H−10, 3H), 3.83 (s, H−9, 3H). ¹³C NMR (125 MHz, CDCl₃) δ: 156.2 (C−7′), 153.7 (C−5), 151.7 (C−2), 147.9 (C−1″), 144.3 (C−4″), 134.0 (C−1′), 130.3 (C−2′), 128.3 (C−3′), 128.0 (C−5′), 127.2 (C−7), 126.9 (C−4′), 125.4 (C−6′), 124.0 (C−1), 123.2 (C−2″), 115.3 (C−3), 114.0 (C−4), 112.6 (C−8), 112.6 (C−3″), 112.1 (C−6), 56.1 (C−9), 55.8 (C−10). HREIMS (TOF-ES⁺) *m/z* 372.1225 [M+Na]⁺ (calculated for $C_{21}H_{19}NO_4Na$: 372.1212).

(E)-N-(2-(2,5-dimethoxystyryl)phenyl)cyclohexane carboxamide (7e): White solid. Yield: 65 %. m.p. 209 ‒ 211 °C. $R_f ≈$ 0.64 [UV-active, *n*-Hexane/EtOAc (Purple spot)]. IR ν$_{max}$: 3249 (N-H), 2914 (C-H), 2850, 1645 (C=O), 1494, 1460, 1279, 1215, 1004, 715. ¹H NMR (500 MHz, CDCl₃) δ ppm: 7.91 (d, *J* = 7.8Hz, H−6′, 1H), 7.53 (d, *J* = 7.8 Hz, H−3′,1H), 7.31 (d, *J* = 17.0 Hz, H−7, H−8, 2H),7.23 (s, N−H, 1H), 7.16 (t, *J* = 8.0 Hz, H−4′, H−5′, 1H), 7.09 (d, *J* = 2.5 Hz, H−6, 1H), 6.87 (d, *J* = 8.8 Hz, H−3, 1H), 6.84 (dd, *J* = 8.8, 2.5 Hz, H−4, 1H), 3.84 (s, H−9, 3H), 3.81 (s, H−10, 3H), 2.29 (m, H−1″, 1H), 2.07−1.95 (m, H−2″, H−6″, 4H), 1.76−1.53 (m, H−3″, H−5″, 4H). ¹³C NMR (125 MHz, CDCl₃) δ ppm: 174.3 (C−7′), 153.7 (C−5), 151.6 (C−2), 134.7 (C−1′), 130.2 (C−2′), 128.2 (C−3′), 127.7 (C−5′), 127.2 (C−7), 126.8 (C−4′), 125.0 (C−6′), 124.4 (C−1), 123.5 (C−3), 114.0 (C−4), 112.3 (C−8), 112.2 (C−6), 56.1 (C−9), 55.8 (C−10), 46.4 (C−1″), 29.8 (C−2″,C−6″), 25.71 (C−4″) 25.6 (C−3″,C−5″). HREIMS (TOF-ES⁺) *m/z* 388.1888 [M+Na]⁺ (calculated for $C_{23}H_{27}NO_3Na$: 388.1889).

(E)-N-(2-(2,5-dimethoxystyryl)phenyl)benzamide (7f): White solid. Yield: 60 %. m.p. 153 – 155 °C. $R_f ≈$ 0.7 [UV-active, *n*-Hexane/EtOAc (Purple spot)]. IR ν$_{max}$: 3294 (N-H), 2924 (C-H), 2830, 1645 (C=O) 1490, 1449, 1215, 1040, 745, ¹H NMR (500 MHz, CDCl₃) δ ppm: 8.06 (d, *J* = 7.5 Hz, H−2″, H−6″, 2H), 7.99 (s, N-H, 1H), 7.92 (d, *J* = 7.5 Hz, H−3″, H−5″, 2H), 7.58 (d, *J* = 7.5 Hz, H−6′, 1H), 7.55 (d, *J* = 7.5 Hz, H−3′, 1H), 7.50 (d, *J* = 15.0 Hz, H−7, H−8, 2H), 7.35 (t, *J* = 7.5 Hz, H−4′, 1H), 7.32 (t, *J* = 7.5 Hz, H−5′, 1H), 7.22 (t, *J* = 7.5 Hz, H−4", 1H), 7.07 (d, *J* = 2.0 Hz, H−6, 1H), 6.85 (d, *J* = 8.5 Hz, H−3, 1H), 6.73 (d, *J* = 8.5 Hz, H−4, 1H) 3.70 (s, H−9, 10, 6H). ¹³C NMR (125 MHz, CDCl₃) δ ppm: 165.7 (C−7′), 153.8 (C−5), 151.7 (C−2), 136.0 (C−1′), 134.9 (C−1″), 132.0 (C−4″), 130.7 (C−2′), 128.9 (C−3″,C−5″), 128.4 (C−3′), 128.3 (C−5′), 127.5 (C−7), 127.2 (C−2″,C−6″), 126.9 (C−4′) 126.8 (C−6′), 125.5 (C−3), 124.6 (C−1), 114.2 (C−4), 112.7 (C−8), 112.2 (C−6), 56.1 (C−9), 55.9 (C−10). HREIMS (TOF-ES⁺) *m/z* 382.1414 [M+Na]⁺ (calculated for $C_{23}H_{21}NO_3Na$: 382.1419).

2.3. Biological Assay

2.3.1. Inhibition of the α-Amylase Enzyme

In this assay, the procedure of Abu Bakar *et al.* was adopted with slight modifications.[22-24] Acarbose, human pancreatic α-amylase, 3,5-dinitrosalicylic acid (DNSA) were purchased. The α-amylase solution was prepared by dissolving 0.025 g of the enzyme in 50 mL phosphate buffer (20 mM, pH 6.9). A colorimetric reagent was prepared by dissolving 3,5-dinitro-salicylic acid (5 g), sodium hydroxide (8 g) and sodium potassium tartrate (150 g) in 350 mL distilled water. The mixture was thoroughly mixed with a magnetic stirrer and the volume was made up to 500 mL with distilled water. To prepare 1% starch solution, 0.25 g of starch was dissolved in 50 mL of sodium acetate buffer (20 mM, pH 6.9) by boiling and continuously stirring for 15 min.

To prepare 500 µg/mL of the stock solution, the appropriate amount of sample was weighed and dissolved in 200 µL acetonitrile in 1% DMSO (2.4 µg/mL). The stock solution was diluted to various concentrations (15.6-250 g/mL) by serial dilution. A sample of 100 µL was added to a tube containing 200 µL of α-amylase solution diluted with starch and 100 µL of 20 mM sodium phosphate buffer (pH 6.9). The solution was pre-incubated at 37 °C for 10 min. Then, about 400 µL of dinitro salicylic acid (DNS) reagent was added to stop the reaction. The tubes were placed in a boiling water bath for 10 min

and afterward cooled to room temperature. Approximately 100 μL of the reaction mixture was then pipetted into a 96-well microplate and the absorbance of the final product was measured at 540 nm using the MPR-96 microplate reader (Halo, Dynamica, Australia). Positive control was prepared using the same method by replacing the sample with th acarbose. The same procedure was used for the negative control, using the buffer instead of the test sample.[22-24] The inhibitory activity of *α*-amylase was determined using the following formula:

$$Percentage\ inhibition\ (\%) = \frac{(Abs.\ control - Abs.\ sample)}{(Abs.\ control)} X\ 100$$

2.3.2. Statistical Analysis

All data are expressed as mean ± SD of triplicate experiments. Statistical analysis was performed by one-way analysis of variance (ANOVA) using GraphPad Prism 5.0. Values of $*p < 0.05$ were considered significant.

2.4. Molecular Docking

Docking methods were used to investigate the binding process at the molecular level to provide a plausible rationale for how the compounds inhibit *α*-amylase. To investigate the interaction affinity, using AutoDock Vina, compounds were sequentially docked to human pancreatic *α*-amylase (PDB ID: 2QV4) to gain better insight into the residual interactions of the most stable ligand-protein complexes formed. Grid scoring was set to maximum or 1, and the RBD region of S was protonated. The $50 \times 50 \times 50$ square grid box was positioned at coordinates of 13.758, 58.583, and 22.465 (x, y, z), respectively. The "view dock" function in UCSF Chimera was used to show the docked complexes, while BIOVIA Discovery Studio Visualizer (2021) was used to examine the interacting residues. [23-25]

3. Results and Discussion

3.1. Chemistry
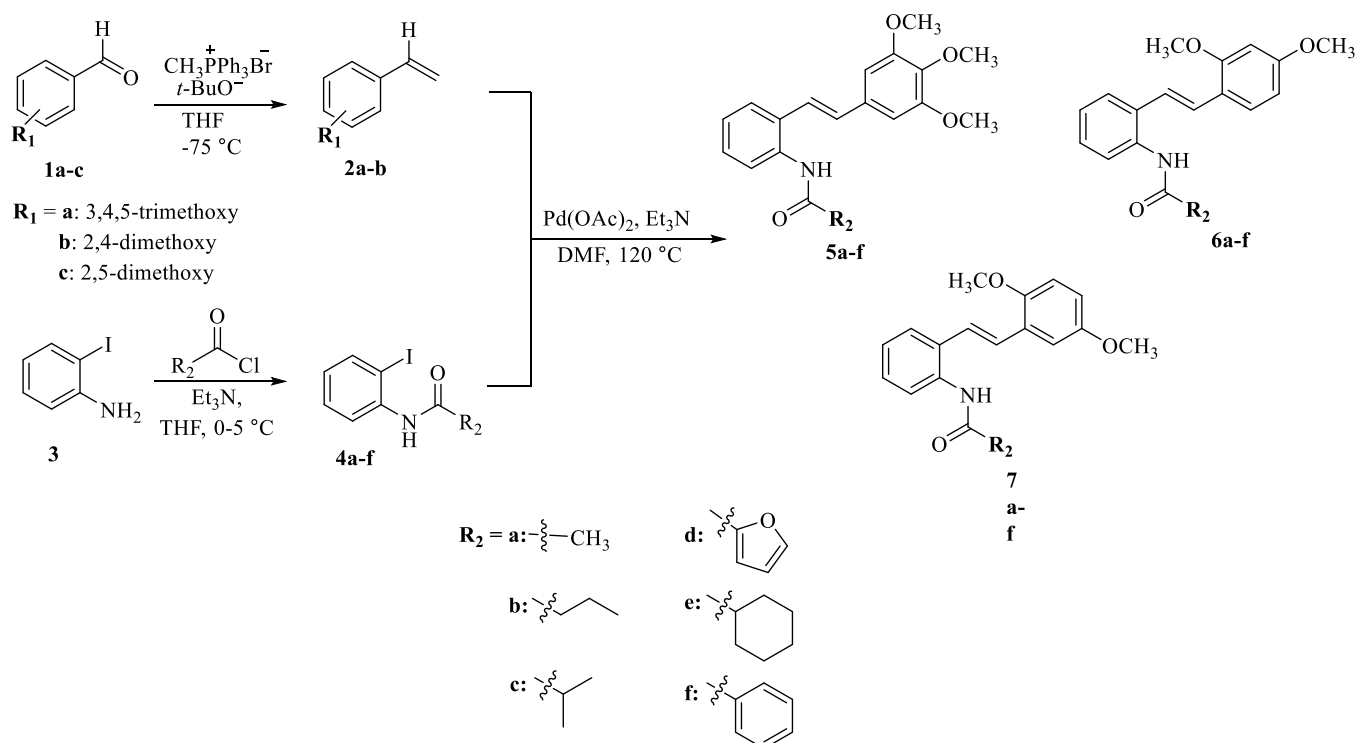
Scheme 1. Synthetic pathway for the preparation of *ortho*-carboxamidostilbene analogues

Synthesis and antidiabetic activity and *in silico* study of *ortho*-carboxamidostilbene analogues

The *ortho*-carboxamidostilbene was synthesized in a two-step process. The intermediate styrene derivatives were synthesized in 89-98% yield by employing the Wittig reaction. Substituted benzaldehydes (**1a-1c**) and methyl triphenyl phosphonium bromide were combined in the presence of *tert*-BuOK to produce styrene derivatives **2a-2c**. Secondly, iodocarboxamide was prepared by reacting 2-iodoaniline in Et$_3$N with respective acyl chloride (at 0–5 °C) to give **4a–4f**. The *ortho*-carboxamidostilbenes were produced in good yield by coupling the iodocarboxamide with styrene **2a–2c** via Heck coupling reaction by using palladium (II) acetate catalyst.[19-21]

In the FT-IR spectra of the synthesized *ortho*-carboxamidostilbenes, it was possible to observe the absorptions between 3215 and 3290 cm^{-1} relating to N–H stretch and absorptions at 1635-1654 cm^{-1} resulting from carbonyl moiety stretching. The ^{1}H NMR spectra for all synthesized compounds show signals for aromatic hydrogens between 6.5 and 8.5 ppm. The signals for vinylic protons of trans olefinic protons, which have larger coupling constants were observed at the same aromatic region with coupling constant between 15.0 to 17.0 ppm. The ^{13}C NMR data of the compounds showed a characteristic peak for C=O at 150-170 ppm. The vinylic carbons of C−7 and C−8 exhibited characteristic peaks at 130-119 ppm, whereas the -OCH$_3$ carbons showed distinct peaks at 56-55 ppm. The HREIMS (TOP-ES$^+$) data indicates the presence of [M+Na]$^+$ ions, as provided in the supplementary file.

3.2. Biological Assay

3.2.1 In-vitro α-Amylase Inhibitory Activity

α-Amylase inhibitory activity of the synthesized compounds **5-7** were performed and compared with acarbose as the reference inhibitor. The results of the α-amylase inhibition assay are presented in Table 1. All synthesized compounds, including reference drug acarbose, were evaluated for their *in vitro* inhibition of α-amylase at different concentrations (15.3−250 μM).

Table 1. α-Amylase inhibitory activity of *ortho*-carboxamidostilbenes **5-7**

Compound	IC$_{50}$ (μM)
5a	33.9 ± 2.2
5b	41.7 ± 0.9
5c	30.7 ± 0.6
5d	40.7 ± 5.1
5e	13.3 ± 0.6
5f	27.9 ± 0.5
6a	33.1 ± 1.4
6b	44.3 ± 6.0
6c	35.7 ± 1.5
6d	34.5 ± 0.4
6e	27.7 ± 0.1
6f	31.6 ± 1.8
7a	31.6 ± 0.5
7b	28.2 ± 0.7
7c	38.6 ± 2.7
7d	30.4 ± 0.5
7e	32.7 ± 6.7
7f	32.5 ± 2.7
Acarbose (control)	30.2 ± 1.9

Results are expressed as mean ± SD (n=3) of at least three independent experiments.

In this series, compounds **5e**, **5f** and **6e** displayed promising inhibition against α-amylase with IC$_{50}$ values ranging from 13.3−28 μM compared with a positive control with an IC$_{50}$ value of 30.2 ± 1.9μM. Based on the obtained results, it could be concluded that compounds **5e** and **6e** with a cyclohexane moiety attached to the amide group at aromatic ring A with methoxy group (at position C−3, C−4 and C−5, IC$_{50}$ = 13.3 ± 0.6 μM, and at position C−2 and C−4, IC$_{50}$ = 27.7 ± 0.1 μM) attached to the benzene ring B exhibited high IC$_{50}$ against α-amylase. Similarly, compound **5f** with three methoxy substituents attached to the aromatic ring B and the phenyl substituent attached to the amide group on aromatic ring A showed a promising IC$_{50}$ against α-amylase with the value of 27.9 ± 0.5 μM.

3.3. Molecular Docking Studies

Molecular docking studies can provide good predictions in molecular modeling analysis, including binding interactions and binding affinity of ligand-receptor complexes. The molecular docking analysis was performed on the four most potent compounds for the *in vitro* α-amylase inhibitory activity (**5e**, **5f**, **6e** and **7b**) against the active site of human pancreatic α-amylase to gain a deeper understanding of their binding interactions. In addition, the standard drug acarbose was also subjected to this docking analysis as the reference. The crystal structure of the diabetic target protein was taken from the RCSB Protein Data Bank with the PDB ID of 2QV4.[23-25] The structure of 2QV4 protein with its active site was selected to control the performance of our docking strategy.[23-25] After the molecular docking process, it was found that all four designed analogues were active against the protein, with the binding energy ranging from -7.5 to -8.7 kcal/mol. The binding energy and docking interactions of these compounds are summarized in Tables 2 and 3, respectively. Besides, the 3D representations of **5e**, **5f**, **6e** and **7b** with their protein interactions are shown in Figure 1(a-d). In comparison to standard drug acarbose, these compounds show significant interactions with the active site of the protein consisting of key amino acids such as Tyr15, Asp19, Trp59, Tyr62, Tyr151, Leu162, Thr163, Leu165, Asp197, Ala198, Lys200, His201, Glu233, Ile235, Asp300 and His305.

Table 2. *In-silico* binding energy between compounds with α-amylase.

Compound	Binding energy (kcal/mol)
5e	-8.7 ± 0.0
5f	-8.3 ± 0.1
6e	-8.6 ± 0.1
7b	-7.5 ± 0.1
Acarbose	-7.8 ± 0.0

Results are expressed as mean ± SD (n=3) of at least three independent experiments.

In general, the docked compounds **5e**, **5f**, **6e** and **7b** were well suited for the α-amylase binding site. They generated a variety of hydrophobic interactions and hydrogen bonds with the embedded amino acid residues. It was found that the major interactions were between the cyclohexane moiety of the ligand and the phenyl group attached to the amide group of ring A with the residues of the enzyme.

In compound **5e** (Figure 1a), TYR151 of the active site residue formed conventional hydrogen bond (distance: 2.05 Å) with the oxygen atom of the methoxy group. The carbon hydrogen bond was also observed between the methoxy group of **5e** and GLU233 of the residues. The π-system of the phenyl rings formed π-cation and π-anion with HIS201 and ASP300, respectively. In addition, similar phenyl rings also established π-π T-shaped interactions with TYR62 and HIS201 which may be due to the planarity of the aromatic rings that create an effective conjugated π-π system with the active site of the amino acid residue. Besides, LEU162 and ILE235 formed a π-alkyl interaction with the also with the phenyl ring whereas LEU165 interacted with the cyclohexyl moiety via alkyl interaction. It was found that the scaffold **5e** with one cyclohexane group and three methoxy group substituents in *meta-* and *para*-position of the phenyl ring was significantly more potent than the other analogues of the synthesized series and the drug acarbose.

Synthesis and antidiabetic activity and *in silico* study of *ortho*-carboxamidostilbene analogues

In the docked **5f** derivative (Figure 1b), the oxygen atom of the two methoxy groups interacted with Tyr151 via conventional hydrogen bonding (2.04 Å and 2.23 Å). Another conventional hydrogen bond (2.79 Å) was also formed between the carbonyl group and HIS101 residue, while additional carbon hydrogen bond was found between the GLU233 residue and -CH₃ moiety of methoxy. Furthermore, the π system of the phenyl group formed π-anion and π-sigma interactions with ASP197 and LEU162, correspondingly.

Table 3. Docking interactions of synthesized compounds within the binding pocket of α-amylase

Compound	Moiety	Residue	Types of interaction
5e	Methoxy	TYR151	Conventional H-bond (2.05 Å)
	Methoxy	GLU233	Carbon H-bond
	Phenyl	HIS201	π-Cation
	Phenyl	ASP300	π-Anion
	Phenyl	TYR62	π-π T-shaped
	Phenyl	HIS201	π-π T-shaped
	Phenyl	LEU162	π-Alkyl
	Phenyl	ILE235	π-Alkyl
	Cyclohexyl	LEU165	Alkyl
	-CH₃	LYS200	van der Waals
5f	-C=O	HIS101	Conventional H-bond (2.79 Å)
	Methoxy	TYR151	Conventional H-bond (2.04 Å)
	Methoxy	TYR151	Conventional H-bond (2.23 Å)
	Methoxy	GLU233	Carbon H-bond
	Phenyl	ASP197	π-Anion
	Phenyl	LEU162	π-Sigma
6e	Methoxy	TYR151	Conventional H-bond (2.31 Å)
	Methoxy	GLU233	Carbon H-bond
	Phenyl	HIS201	π-Cation
	Phenyl	ASP300	π-Anion
	Phenyl	ILE235	π-Sigma
	Phenyl	LEU162	π-Alkyl
	Cyclohexyl	LEU165	Alkyl
7b	-C=O	HIS305	Conventional H-bond (2.65 Å)
	Methoxy	TRP59	π-Sigma
	Phenyl	TRP59	π-π Stacked
	Phenyl	TRP59	π-π Stacked
	Phenyl	TYR62	π-π Stacked
	-CH₃	LEU165	van der Waals

Besides, for compound **6e** (Figure 1c), the TYR151 residue was found to form a conventional hydrogen bonding (2.31 Å) with the negatively charged oxygen of the methoxy group, while GLU233 showed carbon hydrogen bond with the -CH₃ of the methoxy moiety. ILE235 and LEU162 interacted with the phenyl group through π-sigma and π-alkyl interactions, respectively. On the other hand, compound **6e** also showed an alkyl interaction between the cyclohexyl moiety and LEU165, whereas the π system of the phenyl group led to the formation of π-cation and π-anion interactions with HIS 201 and ASP300 residues, correspondingly. In the case of compound **7b** (Figure 1d), the HIS305 residue formed a conventional hydrogen bond (2.65 Å) with the carbonyl group while TRP59 possessed a π-sigma interaction with the -CH₃ of the methoxy group. Likewise, the phenyl groups of **7b** interacted with TRP59 (two interactions) and TYR62 via a π-π stacking, which further enhanced this ligand-receptor intercalation
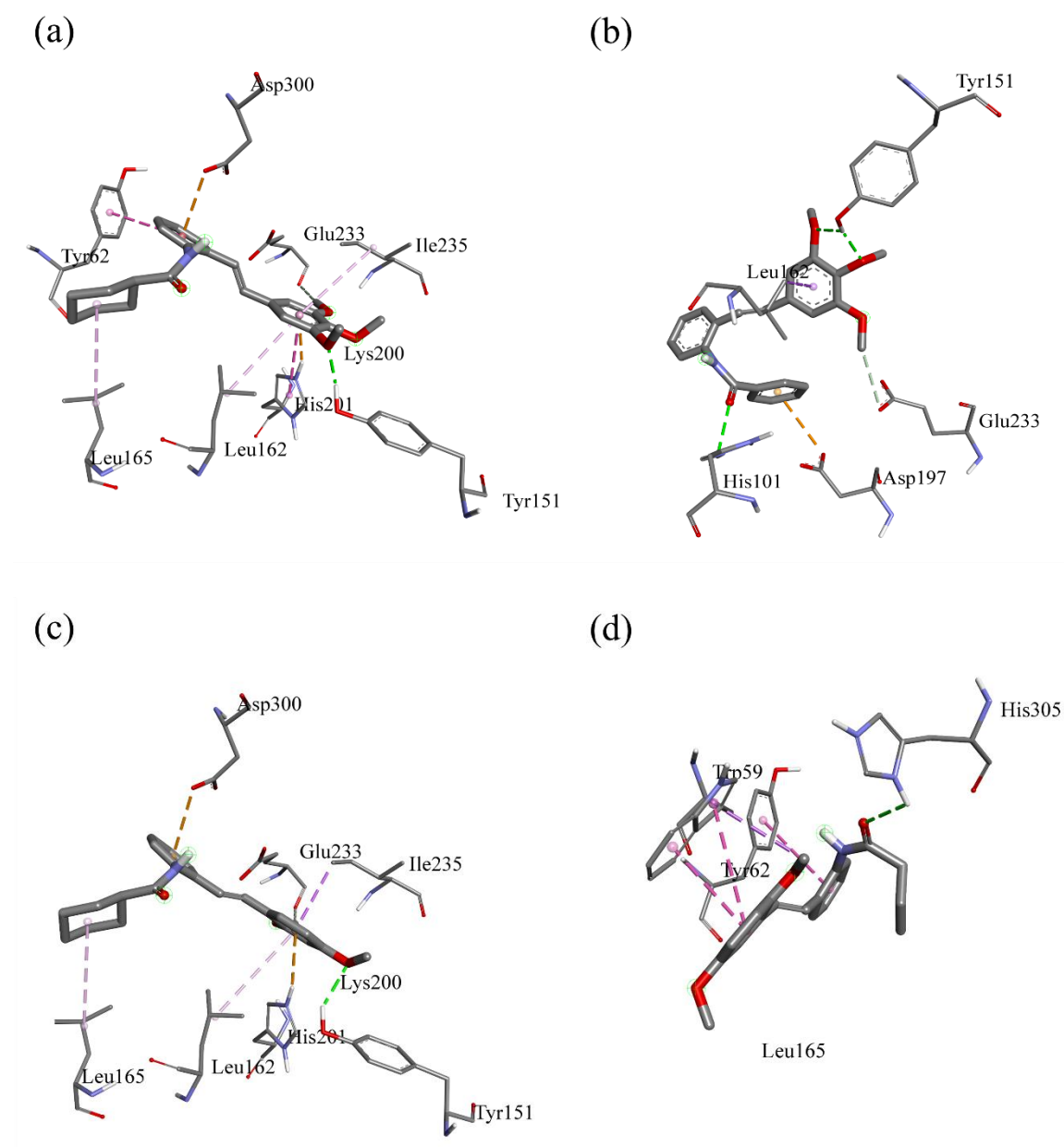

Figure 1. 3D representations of the binding modes of compounds **5e** (a), **5f** (b), and **6e** (c) and **7b** (d) to human pancreatic *α*-amylase (PDB ID: 2QV4)

Synthesis and antidiabetic activity and *in silico* study of *ortho*-carboxamidostilbene analogues

3.4. Structure-Activity Relationship (SAR)

The structure-activity relationship (SAR) of the *ortho*-carboxamidostilbene incorporated with six different moieties were conducted to analyse the impacts of a chemical structure to the potency in inhibiting α-amylase enzymes. The *in vitro* antidiabetic properties of the eighteen *ortho*-carboxamidostilbene were compared with the standard drug acarbose using α-amylase inhibitory activity assay. As shown in Table 1, compounds **5e**, **5f**, **6e** and **7b** have significantly inhibited α-amylase enzymes. Thus, the structural difference of the synthesized *ortho*-carboxamidostilbene derivatives brought significant variation in their antidiabetic activities.

In the first series of 3,4,5-trimethoxy *ortho*-carboxamidostilbene (with 3 methoxy group at *meta-* and *para*-positions), the cyclohexane-substituted *ortho*-carboxamidostilbene derivative of **5e** (IC$_{50}$ = 13.3 $\pm$ 0.6 μM) was the most promising α-amylase inhibitor among all of the synthesized compounds. With around two-fold improvement in the potency compared with positive control acarbose, this is confirmed by the lowest *in silico* binding energy of -8.7 kcal/mol, in contrast to the control with -7.8 kcal/mol. Similarly, the benzyl-substituted stilbene derivative of **5f** showed a considerable inhibitory effect against α-amylase with an IC$_{50}$ value of 27.9 $\pm$ 0.5 μM. Moreover, in the second and third derivatives series, only two compounds (**6e**, IC$_{50}$ = 27.7 $\pm$ 0.1 μM and **7b**, IC$_{50}$ = 28.2 $\pm$ 0.7 μM) show promising α-amylase inhibition. These inhibitory values could be due to the fact that they have two methoxy groups attached to the benzene ring. The mechanisms involved in the inhibitory activity of α-amylase by the derivatives and the positive control might be due to the interactions (hydrogen bond, hydrophobic interactions and van der Waals) with the key amino acids of the enzymes, leading to their inhibitory potential.

Consequently, it was observed that the presence of cyclohexyl and aromatic benzyl substituents linked to the amide moiety can enhance α-amylase inhibitory activity. Figure 2 below summarizes the structural requirements of ortho-carboxamidostilbenes for the suppression of α-amylase activities.
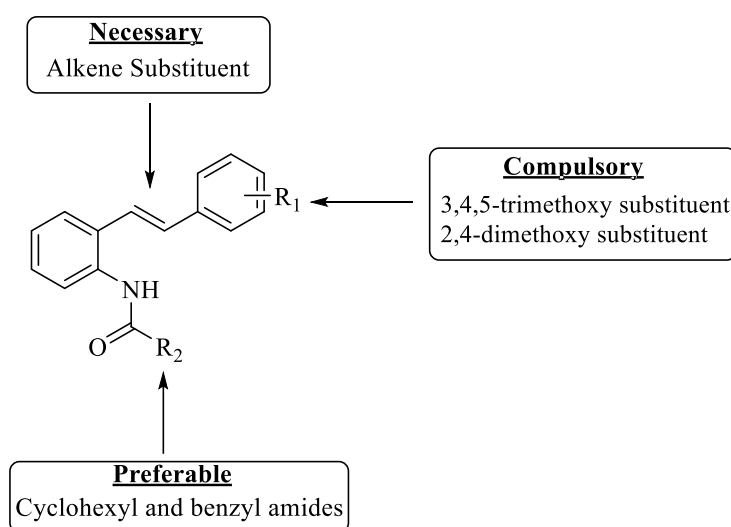

Figure 2. A designed strategy for the SAR studies of *ortho*-carboxamidostilbene derivatives

4. Conclusion

Eighteen new *ortho*-carboxamidostilbene derivatives were synthesized using the Heck coupling reaction. The compounds were obtained with high purity and moderate yield (40 – 77%). Their structure was confirmed using HRMS, FTIR and 1D-NMR techniques. All of these compounds were evaluated for their antidiabetic properties against human pancreatic α-amylase, and the results showed that the most active analogues were **5e**, **5f** and **6e** in comparison to the standard drug acarbose. Among the most active analogues, compound **5e** exhibited the highest potency in inhibiting α-amylase enzymes due to the presence of cyclohexane substituents at the carbonyl carbon of *ortho*-carboxamidostilbene.

Analogues **5f** and **6e** also showed interesting activity with moderate α-amylase inhibition. Moreover, the *in silico* study of the selected potent analogues with the target protein (PDB ID: 2QV4) revealed multiple binding interactions, which correlated to the promising results for the *in vitro* suppression experiment. Noteworthy, our findings indicated that 3,4,5-trimethoxy as well as 2,4-dimethoxy carboxamidostilbene derivatives that were substituted with cyclohexane and phenyl moieties could be the potential lead compounds in the discovery of potent and effective drugs for the treatment of diabetes mellitus.

Acknowledgements

Supporting Information

Supporting information accompanies this paper at http://www.acgpubs.org/journal/organic-communications

ORCID

Babai Mahdi: 0000-0001-8565-0595
Mohamad Nurul Azmi: 0000-0002-2447-0897
Lacksany Phongphane: 0009-0009-0158-6465
Muhammad Solehin Abd Ghani: 0000-0001-8729-2357
Mohamad Hafizi Abu Bakar: 0000-0001-8064-695X
Mohammad Tasyriq Che Omar: 0000-0002-1294-7520
Andrey A. Mikhaylov: 0000-0001-9433-9141
Unang Supratman: 0000-0003-1104-2321

References

[1] Movahed, A.; Nabipour, I.; Lieben Louis, X.; Thandapilly, S. J.; Yu, L.; Kalantarhormozi, M.; Rekabpour, S. J.; Netticadan, T. Antihyperglycemic effects of short-term resveratrol supplementation in type 2 diabetic patients. *Evid. Based. Complement. Alternat. Med.* **2013**, 13, 1-11.

[2] Hussain, F.; Khan, Z.; Jan, M. S.; Ahmad, S.; Ahmad, A.; Rashid, U.; Ullah, F.; Ayaz, M.; Sadiq, A. Synthesis, *in-vitro* α-glucosidase inhibition, antioxidant, *in-vivo* antidiabetic and molecular docking studies of pyrrolidine-2,5-dione and thiazolidine-2,4-dione derivatives. *Bioorg. Chem.* **2019**, *91*, 103128.

[3] Mohamad, N.; Phua, Y. H.; Abu Bakar, M. H.; Che Omar, M. T.; Wahab, H. A.; Supratman, U.; Awang, K.; Azmi, M. N. synthesis, biological evaluation of *ortho*-carboxamidostilbenes as potential inhibitors of hyperglycaemic enzymes, and molecular docking study. *J. Mol. Struct.* **2021**, *1245* (*21*), 131007.

[4] Zeka, K.; Arroo, R. R. J.; Hasa, D.; Beresford, K. J. M.; Ruparelia, K. C. New resveratrol analogues for potential use in diabetes and cancer. *Biomed. J. Sci. Tech. Res.* **2018**, *6* (*2*). 5201-5206.

[5] Khan, I.; Rehman, W.; Rahim, F.; Hussain, R.; Khan, S.; Rasheed, L.; Alanazi, M. M.; Alanazi, A. S.; Abdellattif, M. H. Synthesis and *In Vitro* α-amylase and α-glucosidase dual inhibitory activities of 1,2,4-triazole-bearing bis-hydrazone derivatives and their molecular docking study. *ACS Omega* **2023**, *8* (*25*), 22508–22522.

[6] Fettach, S.; Thari, F. Z.; Hafidi, Z; Karrouchi, K.; Bouathmany, K.; Cherrah, Y.; Achouri, M. El; Benbacer, L.; Mzibri, M. El; Sefrioui, H.; Bougrin, K.; Faouzi, M. E. A. Biological, toxicological and molecular docking evaluations of isoxazoline-thiazolidine-2,4-dione analogues as new class of anti-hyperglycaemic agents. *J. Biomol. Struct. Dyn.* **2023**, *41* (*3*), 1072–1084.

[7] Shafique, K.; Farrukh, A.; Mahmood Ali, T.; Qasim, S.; Jafri, L.; Abd-Rabboh, H. S. M.; AL-Anazy, M. mana; Kalsoom, S. Designing click one-pot synthesis and antidiabetic studies of 1,2,3-triazole derivatives. *Molecules* **2023**, *28* (*7*). 3104-3120.

[8] Bommer, C.; Sagalova, V.; Heesemann, E.; Manne-Goehler, J.; Atun, R.; Bärnighausen, T.; Davies, J.; Vollmer, S. Global economic burden of diabetes in adults: projections from 2015 to 2030. *Diabetes Care* **2018**, *41* (*5*), 963–970.

Synthesis and antidiabetic activity and *in silico* study of *ortho*-carboxamidostilbene analogues

[9]   Toumi, A.; Boudriga, S.; Hamden, K.; Sobeh, M.; Cheurfa, M.; Askri, M.; Knorr, M.; Strohmann, C.; Brieger, L. Synthesis, antidiabetic activity and molecular docking study of rhodanine-substitued spirooxindole pyrrolidine derivatives as novel α-amylase inhibitors. *Bioorg. Chem.* **2021**, *106* (*20*), 104507.

[10]   Mikkel Pape Dysted, B. *IDF Diabetes Atlas 10th Edition*.

[11]   Lu, Q.; Ye, F.; Sun, X.; Weng, J.; Yu, Q.; Hu, D. Design and synthesis of novel nature-inspired stilbene analogues as potential topoisomerase 1 inhibitors. *Chin J Org Chem* **2021**, *41* (8), 3321–3329.

[12]   Michelle, P.; Monteiro, P.; Simeoni, A.; De, P.; Magalhães, O.; Silveira, D. α-Amylase Inhibitors: A review of raw material and isolated compounds from plant source. *J. Pharm. Pharmaceut. Sci.* **2012**, *15*(*1*), 141-183.

[13]   Nickavar, B.; Abolhasani, L. Bioactivity-guided separation of an α-amylase inhibitor flavonoid from *Salvia virgata*. *Iran J. Pharm. Res.* **2013**, *12*(*1*), 57–61.

[14]   Yadav, R.; Prakash B. J.; Kumar V. S.; Kumar N. M. The evaluation of serum amylase in the patients of type 2 diabetes mellitus, with a possible correlation with the pancreatic functions. *J. Clin. Diagn. Res.* **2013**, *7*(*7*), 1291-1294.

[15]   Dayma, V.; Chopra, J.; Sharma, P.; Dwivedi, A.; Tripathi, I.; Bhargava, A.; Vanangamudi, M.; Goswami, A.; Prabhat, K.; Baroliya, P. K. Synthesis, antidiabetic, antioxidant and anti-inflammatory activities of novel hydroxytriazenes based on sulpha drugs. *Heliyon* **2020**, *6* (*8*). e04787.

[16]   Wang, B.; Liu, T.; Wu, Z.; Zhang, L.; Sun, J.; Wang, X. Synthesis and biological evaluation of stilbene derivatives coupled to NO donors as potential antidiabetic agents. *J. Enzym. Inhib. Med. Chem.* **2018**, *33* (*1*), 416–423.

[17]   Özdaş, S.; Taştekin, B.; Gürgen, S. G.; Özdaş, T.; Pelit, A.; Erkan, S. O.; Tuhanioğlu, B.; Gülnar, B.; Görgülü, O. Pterostilbene protects cochlea from ototoxicity in streptozotocin-induced diabetic rats by inhibiting apoptosis. *PLoS One* **2020**, *15* (*7*), e0228429.

[18]   Azmi, M. N.; Sian, T. A.; Suhaimi, M.; Kamarudin, M. N. A.; Din, M. F. M.; Nafiah, M. A.; Thomas, N. F.; Kadir, H. A.; Awang, K. Synthesis of indolostilbene via FeCl₃-promoted oxidative cyclization and their biological effects on NG108-15 cell viability and H₂O₂-induced cytotoxicity. *J. Phys. Sci.* **2021**, *32* (*1*), 69–89.

[19]   Azmi, M. N.; Md Din, M. F.; Kee, C. H.; Suhaimi, M.; Ping, A. K.; Ahmad, K.; Nafiah, M. A.; Thomas, N. F.; Mohamad, K.; Hoong, L. K.; Awang, K. Design, synthesis, and cytotoxic evaluation of *ortho*-carboxamido stilbene analogues. *Int J Mol Sci* **2013**, *14* (12), 23369–23389.

[20]   Kee, C. H.; Ariffin, A.; Awang, K.; Takeya, K.; Morita, H.; Hussain, S. I.; Chan, K. M.; Wood, P. J.; Threadgill, M. D.; Lim C. G.; Ng S.; Weber, J. F. F.; Thomas, N. F. Challenges associated with the synthesis of unusual o-carboxamido stilbenes by the Heck protocol: Intriguing substituent effects, their toxicological and chemopreventive implications. *Org. Biomol. Chem.* **2010**, *8* (*24*), 5646-5660.

[21]   Kee, C. H.; Ariffin, A.; Awang, K.; Noorbatcha, I.; Takeya, K.; Morita, H.; Lim C. G.; Thomas, N. F. Cyclization vs. cyclization/dimerization in o-amidostilbene radical cation cascade reactions: The amide question. *Molecules* **2011**, *16* (*9*), 7267-7287.

[22]   Abu Bakar, M. H.; Lee, P. Y.; Azmi, M. N.; Lotfiamir, N. S.; Faris Mohamad, M. S.; Nor Shahril, N. S.; Shariff, K. A.; Ya'akob, H.; Awang, K.; Litaudon, M. *In vitro* anti-hyperglycaemic, antioxidant activities and intestinal glucose uptake evaluation of *Endiandra Kingiana* extracts. *Biocatal. Agric. Biotechnol* **2020**, *25*, 1-11.

[23]   Phongphane, L.; Mohd Radzuan, S. N.; Abu Bakar, M. H.; Che Omar, M. T.; Supratman, U.; Harneti, D.; A. Wahab, H.; Azmi, M. N. Synthesis, biological evaluation, and molecular modelling of novel quinoxaline-isoxazole hybrid as anti-hyperglycemic. *Comput. Biol. Chem.* **2023**, *106*,107938

[24]   Saad, N. A.; Mohammad, S.; Abu Bakar, M. H.; Che Omar, M. T.; Litaudon, M.; Awang, K.; Azmi, M. N. Anti-hyperglycemic activities, molecular docking and structure-activity relationships (SARs) studies of endiandric acids and kingianins from *Endiandra kingiana*. *J. Braz. Chem. Soc.* **2022**, *33* (*9*), 1017-1027.

[25]   Pettersen, E. F.; Goddard, T. D.; Huang, C. C.; Couch, G. S.; Greenblatt, D. M.; Meng, E. C.; Ferrin, T. E. UCSF Chimera - A visualization system for exploratory research and analysis. *J. Comput. Chem.* **2004**, *25* (*13*), 1605–1612.

ACG

publications